University of Nebraska - Lincoln

DigitalCommons@University of Nebraska - Lincoln

Biological Systems Engineering: Papers and Publications

Biological Systems Engineering

6-2017

Impact of macropores and gravel outcrops on phosphorus leaching at the plot scale in silt loam soils

Derek M. Heeren
University of Nebraska-Lincoln, derek.heeren@unl.edu

Garey A. Fox
North Carolina State University, gafox2@ncsu.edu

Chad Penn
USDA Agricultural Research Service, CHAD.PENN@ARS.USDA.GOV

Todd Halihan
Oklahoma State University - Main Campus, todd.halihan@okstate.edu

Daniel E. Storm
Oklahoma State University - Main Campus, dan.storm@okstate.edu

See next page for additional authors

Follow this and additional works at: https://digitalcommons.unl.edu/biosysengfacpub

Part of the Bioresource and Agricultural Engineering Commons, and the Environmental Engineering Commons

Authors

Derek M. Heeren, Garey A. Fox, Chad Penn, Todd Halihan, Daniel E. Storm, and Brian Haggard

IMPACT OF MACROPORES AND GRAVEL OUTCROPS ON PHOSPHORUS LEACHING AT THE PLOT SCALE IN SILT LOAM SOILS

D. M. Heeren, G. A. Fox, C. J. Penn, T. Halihan, D. E. Storm, B. E. Haggard

ABSTRACT. *In response to increased nutrient loads in surface waters, scientists and engineers need to identify critical nutrient source areas and transport mechanisms within a catchment to protect beneficial uses of aquatic systems in a cost-effective manner. It was hypothesized that hydrologic heterogeneities (e.g., macropores and gravel outcrops) in the vadose zone play an integral role in affecting flow and solute transport between the soil surface and shallow alluvial aquifers. The objective of this research was to characterize phosphorus (P) leaching through silt loam soils to alluvial gravel aquifers in the floodplains of the Ozark ecoregion at the plot scale. Solute injection experiments used plots (1 m × 1 m, 3 m × 3 m, and 10 m × 10 m) that maintained a constant head for up to 52 h. Solutes in the injection water included P (highly sorptive), Rhodamine WT (slightly sorptive), and chloride (conservative). Electrical resistivity imaging identified zones of preferential flow. Fluid samples from observation wells indicated nonuniform subsurface flow and transport. The surface soil type, ranging from silt loam to clean gravel outcrops, had a significant impact on P leaching capacity, with gravel outcrops resulting in high infiltration rates and rapid solute detection in wells (e.g., 4 min). Even in silt loam soils without gravel outcrops, macropore flow resulted in rapid transport of P. Maximum transport velocity for soluble reactive P in one silt loam plot was 810 cm h^{-1}, compared with a mean pore water velocity in the range of 25 to 130 cm h^{-1}. Soluble reactive P concentrations in observation wells reached up to 0.54 mg L^{-1} in silt loam plots and 1.3 mg L^{-1} in gravel outcrop plots, demonstrating that a highly sorbing solute can be mobile.*

Keywords. *Gravel outcrop, Leaching, Macropores, Ozark ecoregion, Phosphorus.*

Increased nutrient loads have adversely influenced surface water quality across the U.S., including excessive algal growth, fish kills, and drinking water taste and odor issues. The significance of this problem has been highlighted by litigation, with one case even reaching the U.S. Supreme Court (Arkansas v. Oklahoma, 1992). Phosphorus (P) is generally considered the limiting nutrient in most surface water systems (Daniel et al., 1998), although nitrogen is critically important to lakes and reservoirs, espe-cially during late summer. While optimum crop growth requires P above 0.2 mg L^{-1} in the soil solution, preventing surface water enrichment generally requires P to be below 0.03 mg L^{-1} in the surface water body (Pierzynski et al., 2005). While surface runoff is considered to be the primary transport mechanism for P, leaching through the vadose zone and subsurface transport to streams (Nelson et al., 2005) may be significant and represents a source of P not alleviated by current conservation practices (e.g., riparian buffers).

Elevated P concentrations in surface water have been a concern in the Illinois River watershed (IRW), which is a trans-boundary watershed within the Ozark Highlands ecoregion of northeastern Oklahoma and northwestern Arkansas. In 2002, the Oklahoma Water Resources Board promulgated a total phosphorus (TP) criterion (i.e., 0.037 mg L^{-1}) for the Scenic Rivers, including the Illinois River, based on Clark et al. (2000). The states of Arkansas and Oklahoma then signed the First Statement of Joint Principles and Actions in 2002, which had state-specific requirements with regard to Oklahoma's TP criterion, wastewater treatment plants (WWTPs), and application of poultry litter to the landscape within the IRW. In 2002, P concentrations, loads, and municipal WWTP inputs started to decrease in the Illinois River as a result of watershed and WWTP management changes (Haggard, 2010; Scott et al., 2011). While concentration reductions closed the gap to Oklahoma's TP criterion, the concentrations during seasonal base flow in summer were still elevated above the criterion in the Illinois River at

The authors are **Derek M. Heeren, ASABE Member,** Assistant Professor and Water for Food Global Institute Faculty Fellow, Department of Biological Systems Engineering, University of Nebraska-Lincoln, Lincoln, Nebraska; **Garey A. Fox, ASABE Member,** Professor and Head, Department of Biological and Agricultural Engineering, North Carolina State University, Raleigh, North Carolina; **Chad J. Penn,** Research Scientist, USDA-ARS National Soil Erosion Research Laboratory, West Lafayette, Indiana; **Todd Halihan,** Professor, School of Geology, and **Daniel E. Storm, ASABE Member,** Professor, Department of Biosystems and Agricultural Engineering, Oklahoma State University, Stillwater, Oklahoma; **Brian E. Haggard,** Professor and Director, Arkansas Water Resources Center, University of Arkansas, Fayetteville, Arkansas. **Corresponding author:** Derek M. Heeren, 241 L. W. Chase Hall, University of Nebraska, Lincoln, NE 68583-0726; phone: 402-472-8577; e-mail: derek.heeren@unl.edu.

the state border (~0.10 mg L^{-1}, B. E. Haggard, unpublished data). The states of Arkansas and Oklahoma agreed to a Second Statement of Joint Principles and Actions requiring a Joint Phosphorus Study to "determine the TP threshold response level at which any statistical shift in algal species composition or algal biomass productions occurs resulting in undesirable aesthetic or water quality conditions in the Designated Scenic Rivers." This Joint Phosphorus Study along with recommendations on TP thresholds, sampling frequency, and sampling duration to state governors will potentially be finished in CY 2016. These legal and regulating actions all point to the importance of understanding P sources and transport pathways within the IRW and the greater Ozark Highlands.

Research is currently limited in understanding the potential significance of connectivity between P in surface runoff and groundwater and P movement from the soil to groundwater in watersheds with cherty and gravelly soils (Fox et al., 2011; Heeren et al., 2011; Mittelstet et al., 2011). While surface runoff is considered to be the primary transport mechanism for P (Gburek et al., 2005), the potential for P leaching is commonly estimated based on point measurements of soil test P (STP) or measurements of the sorption capacity of disturbed soil samples representing the soil matrix. However, in many riparian floodplains, gravel outcrops and macropores are present (Miller et al., 2014). These gravel outcrops can lead to extremely high infiltration rates, some of which are reported to be on the order of 800 cm h^{-1} (Sauer and Logsdon, 2002; Sauer et al., 2005). P-laden water during high-flow discharges exceeding bankfull events can infiltrate in the floodplain subsoil and migrate back to the streams.

Considerable research on P leaching has been performed on the properties of point soil samples, and some research has been conducted on P transport in undisturbed soil columns (West, 1992; Ulen, 1999; Maguire and Sims, 2002; Djodjic et al., 2004). Djodjic et al. (2004) performed experiments on P leaching through undisturbed soil columns and stressed the need to consider larger-scale leaching processes due to soil heterogeneity. They stated that the "water transport mechanism through the soil and subsoil properties seemed to be more important for P leaching than soil test P value in the topsoil. In one soil, where preferential flow was the dominant water transport pathway, water and P bypassed the high sorption capacity of the subsoil, resulting in high losses." P leaching has been monitored under natural field conditions with lysimeters (West, 1992) and vacuum samplers (Nelson et al., 2005), but these methods may not intercept infrequent but important macropores. Field research has been limited on P leaching at the plot scale (1 to 100 m^2), where infiltration and transport may be controlled by heterogeneity present at various scales.

A common best management practice in riparian floodplains is using riparian buffers or vegetative filter strips (VFS) to reduce sediment, nutrient, and pesticide loading to nearby surface water bodies (Popov et al., 2005; Reichenberger et al., 2007; Sabbagh et al., 2009; Fox and Penn, 2013). Reduced transport occurs through contact between dissolved-phase solutes with vegetation in the filter strip and/or by reducing flow velocities to the point where eroded

sediment particles can settle out of the water. In floodplains with significant heterogeneity, such as macroporosity and gravel soils, the effectiveness in preventing loading to nearby streams and rivers may be less than originally anticipated if a significant transport pathway occurs into the shallow groundwater and bypasses the filtering capacity of the VFS. The impact of such heterogeneous infiltration and leaching is not known at this time.

Several studies have been conducted to investigate subsurface P transport in alluvial aquifers in the Ozark ecoregion. Injection tests showed preferential flow paths and physical non-equilibrium in the coarse gravel vadose and phreatic zones (Fuchs et al., 2009; Heeren et al., 2010). Preferential flow paths were interpreted to be buried gravel bars (Heeren et al., 2010; Miller et al., 2014, 2016). Long-term flow and transport monitoring at two floodplain sites showed aquifer heterogeneity and large-scale bank storage of stream water (Heeren et al., 2014b) and stage-dependent transient storage of P in the alluvial aquifer (Heeren et al., 2011). Subsurface P transport rates in the alluvial aquifers were quantified and found to be significant compared to surface runoff P transport rates on well-managed pastures (Mittelstet et al., 2011).

The specific objective of this research was to quantify the impact of hydrologic heterogeneities on the P transport capacity of silt loam soils common in the Ozark ecoregion. Two types of hydrologic heterogeneities were expected to promote greater infiltration and solute transport than initially expected: (1) macropores or large openings (greater than 1 mm) in the soil (Thomas and Phillips, 1979; Akay et al., 2008; Abou Najm et al., 2010) and (2) gravel outcrops at the soil surface (Saur et al., 2005; Miller et al., 2014). Field experiments measured P concentration of water in the gravelly subsoil during ponded infiltration at several alluvial floodplains with varying topsoil thickness.

METHODS

ALLUVIAL FLOODPLAIN SITES

Three alluvial floodplain sites were selected in the IRW, with soils generally consisting of a silt loam mantle underlain with alluvial gravel deposits (table 1). Five infiltration plots at the Barren Fork Creek site were located in two areas based on electrical resistivity imaging data (Miller et al., 2014, 2016): (1) where the gravel formation was under a thick mantle (134 to 145 cm) of silt loam ("deep gravel"), and (2) on a buried gravel bar where the gravel was closer to the current ground surface (104 to 113 cm of silt loam, "shallow gravel"). At the Pumpkin Hollow site, two infiltration plots were located in gravel outcrops, and two were located on control locations without a distinct gravel outcrop. Gravel outcrops in the floodplain appeared to be gravel splays from a recent high-flow event (on the order of a 50-year recurrence interval) rather than an exposed buried gravel bar. Five infiltration plots at the Clear Creek floodplain site were located in two unique geomorphic formations. Formation A, located on the west side of the creek, was very similar to the alluvial deposits at the Barren Fork Creek site, with an apparently uniform layer of silt loam (0.5 to 1.0 m) above chert

Table 1. Location and characteristics of the floodplain sites in the Ozark ecoregion.

	Barren Fork Creek Site	Pumpkin Hollow Creek Site	Clear Creek Site
Nearest city	Tahlequah, Oklahoma	Tahlequah, Oklahoma	Fayetteville, Arkansas
Latitude	35.90°	36.02°	36.13°
Longitude	-94.85°	-94.81°	-94.24°
USDA soil series	Razort gravelly loam	Razort gravelly loam	Razort gravelly loam
Depth of silt loam (cm)	30 to 200	0 to 3	30 to 240
Dry bulk density of silt loam (g cm^{-3})	1.3 to 1.7	1.3 to 1.5	1.5 to 1.7
Land use	Hay field	Pasture	Pasture
STP (mg kg^{-1})	33	120	32[a]

[a] Sampled in Formation A on the west side of the creek.

gravel generally extending downward to limestone bedrock. Unlike the Barren Fork Creek site, the gravel in Formation A contained a buried soil horizon with potential for a perched water table. Formation B, located on the east side of the creek, was very gravelly at the surface but the gravel had a high enough proportion of fines to cause low infiltration rates. The streambank profile at Formation B was 3.5 m tall, with a very thick limiting layer (silt loam) ranging from 2.1 to 2.4 m thick. Further information on the three field sites, including site maps and plot locations, can be found in Heeren et al. (2015).

Background soil P levels were characterized with the Mehlich III soil test P (STP) method (Mehlich, 1984). At each site, 25 to 30 samples were collected with a hand-held soil probe (0-15 cm depth) from random locations in a large area around the infiltration plots. The individual samples were composited and mixed thoroughly. Three replications from each composite sample were tested at the Oklahoma State University Soil, Water, and Forage Analytical Laboratory, with the average STP of the three replicates being the STP for a site (table 1).

SOIL CORES AND CHEMICAL ANALYSIS

Soil core samples were collected with a 6200 TMP (trailer-mounted probe) direct-push drilling machine (Geoprobe Systems, Salina, Kans.) using a dual-tube core sampler with a 4.45 cm opening. The sampler opening (size) limited the particle size sampled from the coarse gravel subsoil; large cobbles occasionally clogged the sampler, resulting in incomplete cores for that depth interval.

Before the P injection experiments, background soil cores were collected during installation of the observation wells from one to four wells per plot. After an experiment was completed, an additional two to four soil cores were collected from within the plot in order to document the change in the soil profile P levels due to the infiltration of P-laden water. Soil cores were stored in the shade during the field experiments (less than six days) and were subsequently refrigerated until the samples could be air-dried and prepared for testing. Geoprobe soil coring typically began at the soil surface and proceeded to, or past, the water table (0.5 to 3.5 m below ground surface). After the 10 m × 10 m plots, a hand soil sampler (0 to 45 cm) was used to take a higher number of samples across the plot.

Soil cores were sliced in the lab into approximately 15 cm samples representing different vertical horizons. All soils were air-dried and sieved with an 8 mm sieve prior to analysis. While a 2 mm sieve is commonly used, laboratory analysis showed that P sorption capacity was significant on the 2 to 4 mm and 4 to 8 mm particle size fractions as well as

the <2 mm size fraction. The >8 mm particle size fraction had only a small capacity for P sorption and was difficult to analyze with regular soil chemistry lab procedures. Therefore, all soil chemistry testing was performed on the <8 mm fraction of each sample.

Soil pH and electrical conductivity (EC) were determined with a 1:1 ratio (mass-based) of soil to de-ionized water solution, stirred with a glass rod and equilibrated for 30 min. All soil samples (approximately 670) were analyzed for water-soluble (WS) P, Al, Fe, Ca, Mg, and Mn content for characterization of P sorption potential. Water extractions were conducted by shaking air-dried soil with de-ionized water (soil:solution ratio of 1:10) end over end for 1 h, followed by centrifuging (2500 rpm at 5 min) and filtration with 0.45 μm Millipore membrane. Extracted P, Al, Fe, Ca, Mg, and Mn were analyzed by inductively coupled plasma atomic emission spectroscopy (ICP-AES).

Oxalate-extractable P, Al, Fe, and Mg (1:40 ratio of soil to 0.2 M acid ammonium oxalate (pH 3), 2 h reaction time in the dark; McKeague and Day, 1966) were determined for all "topsoil" (approximately the top 10 to 15 cm of the soil core) samples ($n = 64$). The P, Al, Fe, and Mg from ammonium oxalate extractions were measured using ICP-AES. The ratio of ammonium oxalate-extractable P to (Al + Fe) (all values in mmol kg^{-1}) was expressed as:

$$DPS_{ox} = \left(\frac{P_{ox}}{Al_{ox} + Fe_{ox}} \right) \times 100 \tag{1}$$

where DPS_{ox} is the ammonium oxalate degree of P saturation (%). Note that this is exactly the same as the traditional soil degree of P saturation (DPS) calculations (Pautler and Sims, 2000) except without the empirical constant α, which is used to relate soil P sorption capacity to Al_{ox} and Fe_{ox}. Because the α value was unknown for these soils, no α value was used (Beauchemin and Simard, 1999; Beck et al., 2004).

Nine P adsorption isotherms were performed on background vadose zone samples (<8 mm fraction) from each geomorphic formation at each site, from various depths, and across a range of textures. The P adsorption isotherms were conducted by adding different levels of P solution (0.0, 0.5, 1.0, 10, and 20 mg P L^{-1}) to 2.0 g soil samples, equilibrating for 24 h (shaking), and measuring P in the equilibrated, centrifuged, and filtered samples with ICP-AES. Because the soil samples already had a significant amount of previously sorbed P, desorption occurred at low solution P concentrations. The equilibrium P concentration (EPC) was calculated as the intercept of a logarithmic trendline fit to the data for each isotherm sample. The EPC is the solution P concentra-

tion at which zero net P sorption or desorption occurs. When the solution surrounding a soil or sediment is greater than its respective EPC, the sediment is expected to adsorb P. If the solution P concentration is less than the EPC, the material is expected to desorb P.

Using a linear least squares model, isotherm data were also fit to the Langmuir equation:

$$s = \frac{bK_L C_{eq}}{1 + K_L C_{eq}} = \frac{k_s C_{eq}}{1 + K_L C_{eq}} \qquad (2)$$

where s is the adsorbed mass (mg P kg^{-1} soil), b is traditionally understood to be the maximum sorption (mg P kg^{-1} soil), K_L is traditionally understood to be the sorption affinity (L water mg^{-1} P), C_{eq} is the equilibrium solution P concentration (mg P L^{-1} water), and k_s is the initial slope of the curve (at low C_{eq}) of the isotherm (L water kg^{-1} soil). While P isotherms are nonlinear and often characterized by the Langmuir equation, they typically exhibit linearity at low concentrations. Therefore, the low C_{eq} data (less than 8 mg L^{-1}) were fit with a linear isotherm:

$$s = K_d C_{eq} + y_{int} \qquad (3)$$

where K_d is the linear sorption coefficient (L water kg^{-1} soil) for the fine fraction (<8 mm) of the soil sample, and y_{int} is where the line intercepts the y-axis (mg P kg^{-1} soil). The absolute value of y_{int} is an indication of the amount of P previously sorbed onto the soil sample at the time of sample collection, although the actual amount of previously sorbed P is likely to be higher due to adsorption-desorption hysteresis.

BERM INSTALLATION AND HYDRAULICS

Measuring leaching of solutes at a plot scale is difficult, especially for high hydraulic conductivity soils. This research used the berm method (Heeren et al., 2014a) to confine infiltration plots and maintain a constant head of 3 to 10 cm of water, with plot sizes ranging from 1 m × 1 m to 10 m × 10 m (fig. 1). Depth to the water table ranged from 50 cm at the Pumpkin Hollow site up to 350 cm at the Clear Creek site. Four to six infiltration experiments were performed at each field site, with plots selected to represent a range of infiltration rates. Specific plot locations and analysis of the infiltration data were presented by Heeren et al. (2015), who found saturated hydraulic conductivity to range over two orders of magnitude.

Each berm was constructed of four sections of 15 cm vinyl hose attached to 90° steel elbows surrounding the infiltration gallery. A shallow trench (3 to 5 cm) was cut through the thatch layer, and a thick bead of liquid bentonite was used to create a seal between the berm and the soil. High-density polyethylene tanks (4.9 and 0.76 m^3) were used to mix stream water and solutes. When a tank was nearly empty, flow was temporarily stopped while the tank was refilled and solutes were added and mixed. Water was gravity-fed to the smaller plots from the mixing tanks, but the largest plots (10 m × 10 m) required continuous pumping from a nearby stream and solute injection directly into the pump hose using Dosatron injectors (D8R, Dosatron, Clearwater, Fla.) (fig. 1).

(a)

(b)

Figure 1. The 10 × 10 infiltration plot at the Clear Creek floodplain site: (a) berm, infiltration gallery, distribution system for water (dyed with Rhodamine WT), and observation wells outside of the plot, and (b) tank with a concentrated solution of solutes and the Dosatron injection system used for large plots.

Chloride (Cl$^-$) was used as a conservative (nonsorbing) tracer. Target tracer concentrations were 100 to 200 mg L^{-1} KCl (correlating to 48 to 95 mg L^{-1} Cl$^-$), depending on background electrical conductivity (EC) levels in the alluvial aquifer. Rhodamine WT (RhWT) was used as a dye introduced into the plots at concentrations of 10 to 100 mg L^{-1}. The RhWT was regarded as a slightly sorbing solute because the soils were expected to have organic matter contents of less than 2%, resulting in a minor amount of RhWT sorption. The RhWT served as a visual indicator of hydraulic connectivity in the observation wells.

The P was expected to be a highly sorbing solute in comparison to Cl$^-$ and RhWT. Target concentrations of 3 to 10 mg L^{-1} (corresponding to 10 to 32 mg L^{-1} as phosphate) were used to represent runoff P concentrations from a field receiving poultry litter (typically used as a fertilizer source in the Ozark ecoregion) in the range of 2 to 8 Mg ha^{-1} (Kleinman et al., 2002; DeLaune et al., 2004; Schroeder et al., 2004). The actual P concentrations in the injection water were 2 to 3 mg L^{-1} for most plots and were achieved by adding phosphoric acid (H$_3$PO$_4$), which deprotonated to H$_2$PO$_4$$^-$

and HPO_4^{2-} in the slightly acidic solution. The inflow water in the plots was sampled throughout the experiment to verify these concentrations. The inflow solution was not buffered because the solution pH remained high relative to the soil pH, which prevented the dissolution of calcium from the soil minerals. The source stream water for injecting was also sampled over time to quantify its P contribution. Redox conditions were not expected to be a concern for characterizing P fate and transport because of the lack of anaerobic conditions due to the high porosity and excessive drainage of both the soil and subsurface materials in Ozark floodplains. For example, dissolved oxygen (DO) of the groundwater at the Barren Fork Creek site measured with a handheld, luminescent-based dissolved oxygen meter (ProODO DO meter, YSI Inc., Yellow Springs, Ohio) ranged from approximately 8 mg L^{-1} near the creek to 4 mg L^{-1} up to 100 m from the creek.

OBSERVATION WELLS AND SAMPLE ANALYSIS

Suction cup lysimeters were not used because of the difficulty of installation in gravelly soils, the risk of creating preferential flow paths in the vadose zone, and the low likelihood of intercepting macropores. Bero et al. (2015) used observation wells to monitor conservative tracers in a shallow aquifer during large plot experiments under rainfall and irrigation. In this research, observation wells were installed every 0.5 to 2 m around the perimeter of the plots to collect groundwater samples. When a confining layer was present (based on soil cores), shallow observation wells were installed, with alternating wells designed specifically to sample from the vadose zone (where perched water was expected) and the remaining observation wells designed specifically to sample from the phreatic zone.

A Geoprobe Systems drilling machine (6200 TMP, Kejr, Inc., Salina, Kans.), which is effective in coarse gravel soils (Heeren et al., 2011; Miller et al., 2011), was used to install 4 to 12 observation wells around each plot. Boreholes were sealed with liquid bentonite to prevent water and solutes from leaking down the annulus. Low-flow sampling with a peristaltic pump (Heeren et al., 2011) was used to collect groundwater samples from the top of the water table (within 10 cm of the water table). Sampling intervals were adjusted based on EC meter readings (to detect elevated levels of Cl^-) and visual observations of RhWT with the goal of having enough data points to characterize solute breakthrough curves.

Well and plot water samples, as well as background stream and groundwater samples, were stored and transported on ice and were tested for both P and Cl^- at the Arkansas Water Resources Center Water Quality Laboratory on the University of Arkansas campus. The soluble reactive P (SRP) samples were filtered within 24 h of sampling using 0.45 µm filters and acidified with sulfuric acid. The SRP was determined colorimetrically with the modified ascorbic acid method (EPA Method 365.2; Murphy and Riley, 1962) with a spectrophotometer (DU 720, Beckman Coulter, Indianapolis, Ind., minimum detection limit of 0.002 mg L^{-1}). The Cl^- concentrations were determined with ion chromatography (minimum detection limit of 0.16 mg L^{-1}). The RhWT samples were analyzed at Oklahoma State University with a Tril-

ogy laboratory fluorometer (Turner Designs, Inc., Sunnyvale, Cal., minimum detection limit of 0.01 mg L^{-1}).

For each solute, the concentration ratio ($C_r = C/C_0$) between the concentration in the well (C) and the concentration injected into the plot (C_0) was used to examine breakthrough curves (BTCs). Without considering macropore and/or gravel outcrop infiltration, P would be expected to only minimally travel through the soil matrix. The BTCs, peak concentrations, and the time to reach the peak concentration in the monitoring wells were compared between the Cl^-, RhWT, and P concentrations, which possess different sorption properties.

It was infeasible to apply an analytical solution of the advection dispersion equation (ADE) to the BTCs for two reasons: (1) dilution of leachate with aquifer water, and (2) transient flow conditions for the solute injection (in contrast to injecting water until steady infiltration was achieved before injecting solutes). Concurrent research is using numerical methods to solve the Richards equation and the ADE with a dual porosity model for this data set (not presented here). In this analysis, solute transport was evaluated by comparing the maximum solute velocity ($v_{s,max}$) to mean pore water velocity (v):

$$v = \frac{q}{\theta} \tag{4}$$

where q is the water flux rate (cm h^{-1}), and θ is the volumetric water content of the soil (cm^3 cm^{-3}). The q value was the steady-state infiltration rate for each plot. The θ value was likely to be near saturation in the upper silt loam layer but much lower in the gravel subsoil. Due to the sharp hydraulic conductivity difference between the silt loam and the gravel, fingering was expected to occur as water from the silt loam percolated into small zones of nearly saturated flow in the high hydraulic conductivity gravel. Therefore, a range of θ was used, resulting in a range of v for each plot. The minimum θ was 0.10, corresponding to the gravel that remained largely unsaturated even during steady ponded infiltration. The maximum θ was 0.50, corresponding to the porosity of the silt loam layer calculated from the minimum dry bulk density (1.3 g cm^{-3}) and assuming a particle density of 2.65 g cm^{-3}.

The maximum solute velocity ($v_{s,max}$) was calculated as the time to initial solute detection in an observation well divided by the distance of travel. The total solute transport distance was the sum of the vertical distance from the soil surface to the water table for each site and the horizontal distance from the edge of the plot to the observation well (50 cm), resulting in a total distance of 350, 100, and 400 cm for the Barren Fork Creek, Pumpkin Hollow, and Clear Creek floodplain sites, respectively. Often an average solute velocity is determined from the breakthrough time, defined as the time when the concentration reaches $0.5C_0$. Because the observation well concentrations rarely reached $0.5C_0$ in this research, the time to the first detection, based on the minimum detection limit for each solute, was used instead. The $v_{s,max}$ based on initial detection was calculated for each solute and plot.

MONITORING WITH ELECTRICAL RESISTIVITY

Vertical electrical resistivity profiles were collected at the floodplain sites during the infiltration and leaching experiments (fig. 2). Electrical resistivity was used to characterize the heterogeneity of the unconsolidated floodplain sediments, as well as locate the infiltrating plume of water and solutes by detecting changes in pore water. Electrical resistivity imaging (ERI) is based on measuring the electrical properties of near-surface earth materials (McNeill, 1980), which vary with grain size, pore-space saturation, pore-water solute content, and electrical properties of the minerals. The electrical behavior of earth materials is controlled by Ohm's law, in which current is directly proportional to voltage and inversely proportional to resistance. Electrical current travels readily in pore water and poorly in air; cations adsorbed to soil particle surfaces reduce resistivity. Clay particles have a large surface area per volume and thus have generally lower resistivity (1 to 100 Ω-m) compared with sands or gravels (10 to 800 Ω-m), which are lower than limestone bedrock (McNeill, 1980).

ERI data were collected using a SuperSting R8/IP earth resistivity meter (Advanced GeoSciences Inc., Austin, Tex.) with 28-electrode arrays. The profiles employed electrode spacings of 0.5 m with an associated depth of investigation of approximately 3 m, which included the vadose zone as well as the top of the water table. The resistivity data from the SuperSting R8/IP were inverted using a proprietary routine devised by Halihan et al. (2005), which produced higher-resolution images than conventional techniques (Heeren et al., 2010; Miller et al., 2014). The ERI resistivity data were interpolated into grids and contoured using Surfer 8 (Golden Software, Inc., Golden, Colo.). Differencing was used to display the percent difference in resistivity between the background image (before infiltration) and images collected during the infiltration experiments. The upgradient electrical resistivity line went through the center of the infiltration plots (fig. 2). The downgradient line was parallel to the first line but 3 m to the southwest, designed to capture the solute plume moving downgradient in the groundwater.

RESULTS AND DISCUSSION
SOIL CHEMICAL PROPERTIES

Isotherms were performed on soil samples displaced from observation well installation, i.e., on soil samples collected before the P injection experiment occurred at that location. The EPC ranged from 0.38 to 3.09 mg L^{-1} and was positively correlated ($R^2 = 0.69$) to WSP (table 2). The P injection solutions for most plots had P concentrations from 2 to 3 mg L^{-1}. Most soil samples had EPC values of less than 2 mg L^{-1}, so net P sorption was expected to occur, with P desorption occurring only minimally during injection field experiments. Because these alluvial aquifers usually possess P concentrations of less than 0.1 mg L^{-1}, these high EPC values indicated that the vadose zone is likely a source of P to the alluvial aquifers under natural rainfall events when deep percolation occurs, even without poultry litter on the soil surface.

The Langmuir equation did not fit the isotherm data well due to the net desorption that occurred with low input P solutions (resulting in negative s), especially on soil samples with high EPC. The K_L and b data were not used as an indication of chemical mechanisms but were considered as fitting parameters. The K_L ranged from 0.003 to 0.083 L mg^{-1}, and the b ranged from 250 to 2200 mg kg^{-1}. The linear equation fit the low concentration data ($C_{eq} < 8$ mg L^{-1}) well, with K_d ranging from 2.6 to 37 L kg^{-1}. The K_d was inversely related to EPC (table 2). In previous research, topsoil samples from both the Clear Creek and Barren Fork Creek sites were analyzed with flow-through P sorption isothermal titration calorimetry (ITC) experiments (Penn et al., 2014). Results showed that the dominant P sorption reaction was ligand exchange onto Al/Fe oxides/hydroxides, with a lesser degree of precipitation, and P removal for both soils was limited by physical nonequilibrium instead of chemical nonequilibrium (sorption kinetics).

Both water-soluble extractions and ammonium oxalate extractions (table 3) were performed on all topsoil samples (approximately the top 10 to 15 cm of the soil core). Soil cores were taken during well installation (before the infiltration experiments) and inside the plot (after the infiltration experiments) in order to compare soil P concentrations before and after the injection of P-laden water (table 3). The WSP concentrations ranged from 1.8 to 15.5 mg kg^{-1}. For some plots, there was a significant increase in WSP from before to after in the infiltration experiment (e.g., the Clear Creek 10×10 plot); however, some plots showed a decrease, which was likely due to the small number of replicates in samples from the plots. On average, the oxalate-extractable P increased by 18, 51, and 54 mg kg^{-1} in the topsoil at the Barren Fork Creek, Pumpkin Hollow, and Clear Creek sites, respectively. The DPS$_{ox}$ ranged from 6.9% to 27.2% and showed a more consistent trend of increase due to the infiltration experiments than WSP.
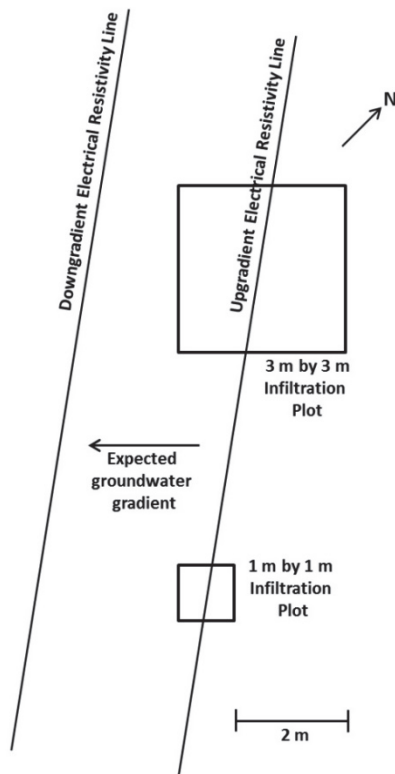

Figure 2. Electrical resistivity design for the deep gravel plots at the Barren Fork Creek site.

Table 2. Soil physical and chemical properties for samples selected for phosphorus adsorption isotherms. All soil chemical tests were performed on the fraction of the soil sample that passed through an 8 mm sieve. The geomorphic formation applies to the plot, but the soil type describes the tested soil sample for the specific borehole and depth below the ground surface.

Soil Physical Characteristics and Isotherms

Site	Plot[a]	Borehole	Sample Depth (cm)	Geomorphic Formation	Soil Type	8 mm Sieve (% retained)	EPC[b] (mg L^{-1})	K_d[c] (L kg^{-1})	y_{int}[d] (mg kg^{-1})
Barren Fork	1×1α	Well B	64 to 83	Shallow gravel	Silt loam, some gravel	6	0.94	11	-14
	3×3α	Well K	142 to 163	Shallow gravel	Sandy gravel	43	1.08	2.6	-6
	1×1β	Well C	74 to 90	Deep gravel	Silt loam	0	0.77	15	-14
Pumpkin Hollow	3×3α	Well T	0 to 17	Outcrop	Silt loam, some gravel	6	0.73	9.8	-10
	1×1β	Well D	78 to 105	Outcrop	Gravel, some sand	53	0.69	11	-10
	3×3β	Well J	40 to 80	Control	Gravelly silt loam	26	0.71	12	-11
Clear Creek	1×1α	Well C	156 to 175	Formation A	Gravel, some sand	56	3.09	37	-118
	3×3α	Well I	39 to 63	Formation A	Silt loam, some gravel	5	0.38	19	-7
	3×3β	Well O	64 to 83	Formation B	Silt loam	-	1.70	8.2	-20

Soil Chemical Properties

Site	Plot	Borehole	Sample Depth (cm)	pH	Electrical Conductivity (µS cm^{-1})	P	Al	Fe	Ca	Mg	Mn
								Water-Soluble Elements (mg kg^{-1})			
Barren Fork	1×1α	Well B	64 to 83	6.3	26	2.8	799	113.1	74	18	2.7
	3×3α	Well K	142 to 163	6.4	10	2.7	321	89.4	17	10	1.7
	1×1β	Well C	74 to 90	6.4	23	2.3	381	106.7	64	16	2.2
Pumpkin Hollow	3×3α	Well T	0 to 17	6.5	148	5.5	250	116	102	22	1.5
	1×1β	Well D	78 to 105	7.3	37	3.2	419	184	65	24	3.3
	3×3β	Well J	40 to 80	6.9	37	2.1	209	97	35	12	1.0
Clear Creek	1×1α	Well C	156 to 175	6.8	10	7.6	2561	586.7	64	61	1.1
	3×3α	Well I	39 to 63	6.2	35	1.4	139	55.4	19	6	1.0
	3×3β	Well O	64 to 83	6.2	13	5.6	331	163.4	20	17	1.5

[a] α and β indicate the first and second set of infiltration experiments performed at a field site.
[b] EPC = equilibrium P concentration.
[c] K_d = linear sorption coefficient.
[d] y_{int} = y-intercept of the linear isotherm.

Table 3. Soil chemical properties for the topsoil (approximately the top 10 to 15 cm of the soil core) at each plot location for both before and after the water and solute infiltration experiments. Data include electrical conductivity (EC) and degree of P saturation (DPS$_{ox}$), which was calculated based on the molar concentrations of the ammonium oxalate extract.

Site	Plot	P Injection	n	pH	EC (µS cm^{-1})	P	Al	Fe	Ca	Mg	Mn	P	Al	Fe	Mg	DPS$_{ox}$ (%)
						Water-Soluble Elements (mg kg^{-1})						Ammonium Oxalate (mg kg^{-1})				
Barren Fork Creek																
	1×1α	Before	2	6.3	97	4.6	192	40	41	9	1.3	223	621	2,050	101	12.0
		After	1	6.3	325	7.5	71	39	123	18	2.4	300	604	2,296	160	15.3
	3×3α	Before	2	6.5	139	5.2	321	66	39	12	2.0	246	704	2,535	102	11.1
		After	3	6.5	134	4.9	198	52	51	10	1.0	269	643	2,373	129	13.1
	1×1β	Before	2	6.0	129	3.3	108	35	81	11	2.2	223	714	2,691	140	9.7
		After	2	6.4	91	3.8	209	57	38	10	0.8	233	669	2,765	90	10.1
	3×3β	Before	2	6.1	112	3.0	95	42	86	11	1.3	230	674	2,647	119	10.3
		After	2	6.3	139	1.8	202	43	32	7	1.0	204	570	2,388	90	10.3
	10×10	Before	1	6.1	93	5.7	90	45	87	14	2.8	246	706	2,486	176	11.2
		After	6	6.1	97	6.8	137	67	65	14	2.2	252	687	2,424	148	11.8
Pumpkin Hollow																
	1×1α	Before	2	6.3	87.2	11.1	212	100	66	19	3.9	163	604	1,252	106	11.8
		After	1	6.5	159	15.5	206	105	89	24	3.5	268	582	1,676	187	16.8
	3×3α	Before	2	6.8	102.3	5.2	353	168	98	26	4.4	129	582	1,439	87	8.6
		After	2	7.0	88.5	4.0	251	129	87	20	3.0	56	286	764	43	7.2
	1×1β	Before	3	6.4	99.6	5.8	197	119	89	19	4.9	160	601	8,846	105	7.7
		After	1	6.2	182	3.6	152	74	104	16	4.4	179	627	1,740	100	10.6
	3×3β	Before	1	6.8	43	2.2	203	92	55	14	1.4	89	649	986	64	6.9
		After	2	6.2	318.5	11.5	157	76	123	19	2.4	240	712	1,399	145	15.0
Clear Creek																
	1×1α	Before	1	5.4	242	1.9	73	32.5	38	9	0.8	196	630	1,724	114	11.7
		After	2	6.0	107.1	3.4	61.6	28.5	37	7	1.0	247	855	1,918	114	12.0
	3×3α	Before	2	5.4	306.1	3.8	62.5	27.9	89	18	1.8	276	804	1,767	221	14.9
		After	2	5.5	240.2	1.3	68.8	31.6	65	11	0.8	235	767	1,929	146	12.1
	1×1β	Before	1	5.8	101	9.2	55	32.0	42	7	3.3	280	900	1,054	92	17.3
		After	2	6.5	120.4	7.0	122.3	67.9	39	8	3.0	427	1064	1,757	102	19.5
	3×3β	Before	3	5.9	79.0	13.0	51.2	25.7	36	8	3.2	455	1120	1,213	141	22.9
		After	2	6.5	137.4	8.5	528.0	301.7	42	39	2.0	515	1042	1,250	118	27.2
	10×10	Before	2	5.9	48.1	3.3	137.1	79.2	46	11	3.1	196	740	1,998	114	9.8
		After	5	6.1	122.9	5.9	92.7	48.8	71	9	3.0	251	737	2,139	113	12.4

OBSERVATION WELL SOLUTE CONCENTRATIONS

Rhodamine WT and Cl⁻ were observed in no wells for some plots and in all wells for other plots; detection of P ranged from no wells to nearly half of the wells for a given plot (table 4). Response times ranged from 0.07 h to greater than 48 h. Infiltration and leaching appeared to correlate weakly to topsoil thickness and stream order. P transport did not correlate significantly with the size of the plot, indicating that all plot sizes were within the representative elementary volume (REV) for measuring P transport.

The time to the first detection (table 5) was as low as 0.07 h for RhWT and 0.13 h for Cl⁻ and SRP (Pumpkin Hollow, 1×1β plot). These low response times, together with the high infiltration rates, demonstrated the impact of the gravel outcrops on the 3×3α and 1×1β plots at the Pumpkin Hollow site (tables 4 and 5). Although RhWT is a slightly sorbing solute, it was occasionally detected before Cl⁻ (a conservative tracer) because RhWT injection concentrations were several orders of magnitude above the minimum detection limit. The velocity ratio indicated the impact of macropores by considering the response time in relation to the infiltration rate (table 5). In many cases, the $v_{s,max}$ was more than double the v, with velocity ratios up to 11. The Barren Fork Creek 3×3α plot had an order of magnitude difference between $v_{s,max}$ and v for all solutes. This included SRP, a highly sorbing solute, which indicates the dramatic impact of macropore flow.

The BTCs showed that C_r began at background levels (near zero) and generally increased with time, approaching

Table 4. Summary of leaching experiments performed at three alluvial floodplain sites in the Ozark ecoregion. The number of wells at each plot containing conservative (Cl⁻), slightly sorbing (Rhodamine WT), and highly sorbing (phosphorus) solutes indicates the capacity for solute transport at that location.

Site	Date	Plot	Geomorphic Formation	Duration of Infiltration (h)	Steady-State Infiltration (q, cm h⁻¹)	Total Wells	Number of Wells Containing: Cl⁻	RhWT[a]	SRP[a]
Barren Fork									
	30 June 2011	1×1α	Shallow gravel	22	10	5	5	5	2
	30 June 2011	3×3α	Shallow gravel	22	13	12	10	10	3
	13 July 2011	1×1β	Deep gravel	46	6.8	4	1	1	0
	13 July 2011	3×3β	Deep gravel	48	3.0	12	5	5	0
	7 May 2012	10×10	Shallow gravel	4	13	14	13	-	5
Pumpkin Hollow									
	4 May 2011	1×1α	Control	32	5.3	8	3	4	3
	5 May 2011	3×3α	Gravel outcrop	2.8	18	12	5	8	5
	1 June 2011	1×1β	Gravel outcrop	4.3	74	4	4	4	1
	2 June 2011	3×3β	Control	24	6.3	12	-[b]	0	-[b]
Clear Creek									
	12 April 2011	1×1α	Formation A	41	5.6	4	-[c]	4	0
	12 April 2011	3×3α	Formation A	41	3.3	8	-[c]	4	2
	27 July 2011	1×1β	Formation B	48	1.3	8	0	0	0
	27 July 2011	3×3β	Formation B	45	0.8	12	0	0	0
	21 May 2012	10×10	Formation A	52	0.6	14	5	-	0

[a] RhWT = Rhodamine WT; SRP = soluble reactive phosphorus.
[b] Not measured because RhWT was not detected.
[c] Cl⁻ added but not sufficiently above background concentrations in the stream and groundwater.

Table 5. Solute transport velocities compared with mean pore water velocity. The velocity ratio is the ratio of the solute velocity to the expected pore water velocity, calculated as the average of the minimum and maximum estimates of pore water velocity.[a]

Site	Plot	Steady-State Infiltration (q, cm h⁻¹)	Mean Pore Water Velocity (v, cm h⁻¹) Min.	Max.	Time to First Detection (h) Cl⁻	RhWT	SRP	Maximum Solute Velocity ($v_{s,max}$, cm h⁻¹) Cl⁻	RhWT	SRP	Velocity Ratio Cl⁻	RhWT	SRP
Barren Fork													
	1×1α	10	20	100	0.83	1	18.6	420	350	19	6.9	5.7	0.3
	3×3α	13	25	130	0.43	0.45	0.43	810	780	810	11	10	11
	1×1β	6.8	14	68	7.25	11.7	>46	48	30	-	1.2	0.7	-
	3×3β	3.0	6	30	6.97	6.97	>46	50	50	-	2.8	2.8	-
	10×10	13	27	130	1.92	-	3.93	180	-	89	2.3	-	1.1
Pumpkin Hollow													
	1×1α	5.3	11	53	13.3	13.3	13.3	8	8	8	0.2	0.2	0.2
	3×3α	18	36	180	0.58	0.5	0.58	170	200	170	1.6	1.9	1.6
	1×1β	74	147	740	0.13	0.07	0.13	750	1500	750	1.7	3.4	1.7
	3×3β	6.3	13	63	-[b]	>24	-[b]	-	-	-	-	-	-
Clear Creek													
	1×1α	5.6	11	56	-[c]	3.5	>41	-	110	-	-	3.4	-
	3×3α	3.3	7	33	-[c]	4	8	-	100	50	-	5.0	2.5
	1×1β	1.3	3	13	>48	>48	>48	-	-	-	-	-	-
	3×3β	0.8	2	8	>45	>45	>45	-	-	-	-	-	-
	10×10	0.6	1	6	26.0	-	>45	15	-	-	4.2	-	-

[a] RhWT = Rhodamine WT; SRP = soluble reactive phosphorus.
[b] Not measured because RhWT was not detected.
[c] Chloride added but not sufficiently above background concentrations in the stream and groundwater.

unity for Cl⁻ in some cases (fig. 3). Within a well, the Cl⁻ (conservative) BTC generally began first, followed by RhWT (slightly sorbing), and finally P (highly sorbing) (fig. 3, table 6). Previous flow-through experiments coupled with calorimetric measurements (Penn et al., 2014) conducted on thin-membrane soils also indicated that both the Barren Fork and Clear Creek soils were able to sorb appreciable P under flowing conditions with short contact times (3 and 10 min).

Observation wells were placed in both the phreatic zone and the vadose zone due to confining layers at the Pumpkin Hollow site and Formation B of the Clear Creek site. Sample collection for the wells in the vadose zone was not possible until a sufficient level of water had perched, at which point
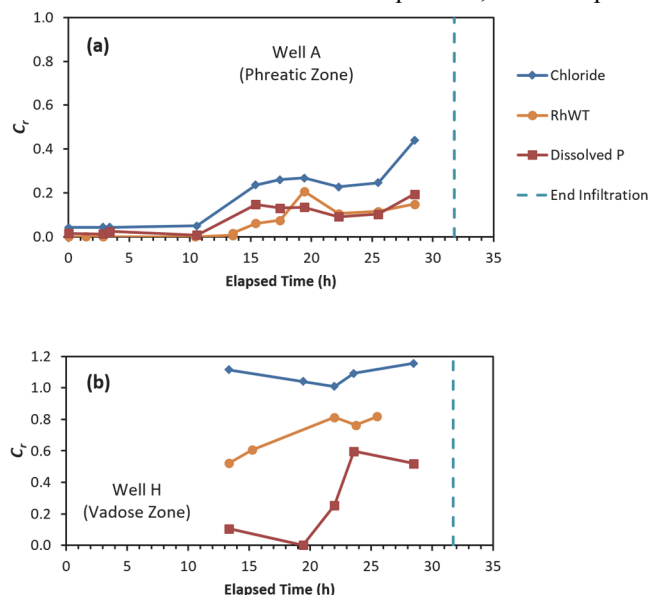
Figure 3. Concentration ratio (C_r) for two of the observation wells during the infiltration experiment for the 1×1α plot at the Pumpkin Hollow floodplain site. Water and solute injection began at 0 h and ended at 31.8 h (indicated by the dashed line).

concentrations were usually high (fig. 3b, table 6). While significant dilution with groundwater occurred in the phreatic zone wells, dilution in the vadose zone wells was expected to be limited to displaced water from the unsaturated zone, resulting in a C_r near 100% for a conservative tracer. During the 5 May 2011 leaching experiment at the Pumpkin Hollow site (3×3α), RhWT leached through the vadose zone and moved laterally 14 m to the stream in less than 1.7 h. The C_r of RhWT in the stream near the seep face reached 0.02 (table 6).

At the Pumpkin Hollow 3×3β plot, 1.5 m of infiltration occurred over 24 h. Using a maximum θ of 0.5, the water would have traveled at least 3 m during the leaching experiment. With a total travel distance of 1.5 m from the infiltration plot to the wells, the infiltrating water must have moved laterally beyond the wells. However, RhWT was never observed in any of the 12 observation wells, with the wells in the phreatic zone spaced from 2 to 3 m apart. The flow must have occurred preferentially at a small enough scale to flow between the well spacing. It was very unlikely that RhWT sorption to organic matter was sufficient to reduce concentrations to below the minimum detection limit, since RhWT is only slightly sorbing and the injection solution had RhWT over three orders of magnitude higher than the minimum detection limit.

For the Barren Fork Creek shallow gravel plots (1×1α and 3×3α), the RhWT and Cl⁻ concentrations increased by the second sample after the start of the experiment, which was approximately 2 h after the initiation of leaching. Slight increases in concentrations of both RhWT and Cl⁻ were observed after the first sample in some wells, which was taken approximately 0.5 to 1 h after the start of the experiment. Groundwater concentrations reached approximately 50% of the injected Cl⁻ concentration at a breakthrough time of less than 2 h from the initiation of infiltration. Because the leaching experiments at the Barren Fork Creek site were not on gravel outcrops (the "shallow gravel" plots had 104 to

Table 6. Transport data by well for the 1×1α (control, 32 h duration) and 3×3α (gravel outcrop, 2.8 h duration) plots at the Pumpkin Hollow floodplain site.[a]

Plot	Well	Zone	Detection Time (h)			Time to Peak (h)			Peak Concentration Ratio (C_r)		
			Cl⁻	RhWT	SRP	Cl⁻	RhWT	SRP	Cl⁻	RhWT	SRP
	A	Phreatic	15	14	15	>29	19	>29	0.44	0.21	0.19
	B	Vadose	26	14	26	29	>29	>29	1.04	0.35	0.21
	C	Phreatic	>29	>29	>29	>29	>29	>29	-	-	-
1×1α	D	Vadose[b]	-	-	-	-	-	-	-	-	-
	E	Phreatic	>29	>29	>29	>29	>29	>29	-	-	-
	F	Vadose[b]	-	-	-	-	-	-	-	-	-
	G	Phreatic	>29	26	>29	>29	26	>29	-	0.001	-
	H	Vadose	13	13	13	29	>26	24	1.16	0.82	0.60
	I	Vadose	0.7	0.5	0.8	1.4	0.8	0.8	0.51	0.49	0.03
	J	Phreatic	>3.1	0.7	>3.1	>3.1	0.8	>3.1	-	0.0003	-
	K	Vadose[b]	-	-	-	-	-	-	-	-	-
	L	Phreatic	>3	0.7	>3	>3	1.1	>3	-	0.004	-
	M	Vadose[b]	-	-	-	-	-	-	-	-	-
	N	Phreatic	0.6	0.6	0.6	1.5	0.8	0.8	0.58	0.28	0.06
3×3α	O	Vadose	1.0	0.7	1.0	>1.0	>1.0	>1.0	0.67	0.36	0.14
	P	Phreatic	>2.9	0.7	>2.9	>2.9	2.9	>2.9	-	0.01	-
	Q	Vadose	1.1	0.6	1.1	2.2	>1.8	>3.0	0.75	0.32	0.30
	R	Phreatic	>2.9	>2.9	>2.9	>2.9	>2.9	>2.9	-	-	-
	S	Vadose	0.8	<1.1	0.8	0.8	1.1	1.6	0.80	0.40	0.13
	T	Phreatic	>2.9	>2.9	>2.9	>2.9	>2.9	>2.9	-	-	-
	Seep	Stream	>2.9	1.7	>2.9	>2.9	2.3	>2.9	-	0.02	-

[a] RhWT = Rhodamine WT; SRP = soluble reactive phosphorus.
[b] Remained dry.

113 cm of silt loam overlying the gravel), this finding indicated the importance of macropore flow in silt loam soils. The P transport was also significant for these two Barren Fork Creek plots (1×1α and 3×3α; table 4). The SRP concentration in well P was 0.28 mg L^{-1} (C_r = 0.16) only 0.43 h after initiation of infiltration. Peak SRP concentrations ranged from 0.16 to 0.54 mg L^{-1} (C_r = 0.30) for the five wells that had detectable SRP (among 17 wells total; table 4). The importance of macropore flow observed in the transport data was consistent with the flow data analyzed by Heeren et al. (2015), who compared tension infiltrometer data with saturated hydraulic conductivity estimated from the plot infiltration data; macropore flow accounted for approximately 84% to 99% of total saturated hydraulic conductivity.

Spatial variability in the flow and transport data was significant. Advection along the regional groundwater gradient generally resulted in higher concentrations on the downgradient side of the plots (fig. 4). The soils in the alluvial floodplain were extremely heterogeneous, which corroborates previous research (Miller et al., 2014, 2016). Even wells only 1 m apart showed significant variation in Cl⁻ (fig. 4).

ELECTRICAL RESISTIVITY IMAGING OF INFILTRATION PLUME

Transient electrical resistivity results showed downward (fig. 5) and lateral (fig. 6) migration of the water and Cl⁻ plume for the Barren Fork Creek deep gravel plots (1×1β and 3×3β). The Cl⁻ was detected in fluid samples from the water table (3 m below ground surface) only 7 h after the initiation of infiltration for both plots, yet the ERI data showed only 1 to 2 m of infiltration after 19 h (fig. 5). This indicates that rapid flow and transport may be occurring in macropores, which only represent a small volume of the soil column, possibly escaping detection by the electrical resistivity equipment. It is also possible that the gravel remained mostly unsaturated (except for fingering) while transporting all the water delivered to it by the silt loam (top 1 m of the soil profile). The downgradient electrical resistivity line showed lateral migration of water and solutes in the vadose zone as well as the phreatic zone (figs. 2 and 6). A traditional understanding of vadose zone hydrology for a silt loam over a gravel layer would not predict lateral movement above the water table, but these data indicate the presence of preferential flow pathways resulting in horizontal transport.

CONCLUSIONS

Highly heterogeneous flow and transport indicated that the soils in the floodplains of the Ozark ecoregion are highly complex and not homogeneous. Elevated Cl⁻, RhWT, and P concentrations were observed in groundwater samples. With injection P concentrations simulating runoff from a field with poultry litter, SRP concentrations in the observation wells reached up to 0.54 mg L^{-1} in silt loam soils and 1.3 mg L^{-1} in gravel outcrops, showing that a highly sorbing solute can be transported through the topsoil and the gravelly subsoils. The impact of gravel outcrops was shown by high infiltration rates (up to 74 cm h^{-1}) and low time to solute detection (down to 4 min). Even in silt loam soils without gravel outcrops, macropore flow resulted in rapid transport of solutes. The impact of macropores was demonstrated by high velocity ratios.
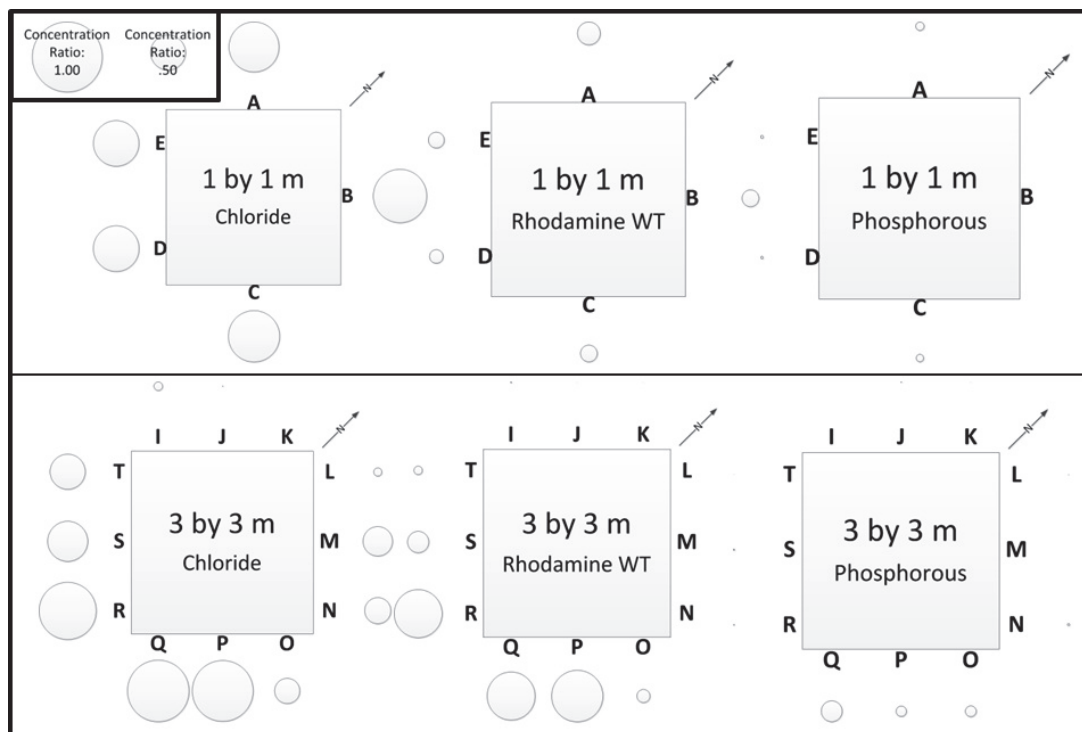

Figure 4. Maximum concentration ratios for samples from each well for the Barren Fork Creek shallow gravel plots (1×1α and 3×3α). Note that the plots are not drawn to scale. The size of the circle around each well represents the concentration ratio. Concentrations were determined from groundwater samples that were collected from the top of the water table, approximately 3 m below the ground surface. The dominant groundwater direction was to the southwest (down the creek valley).
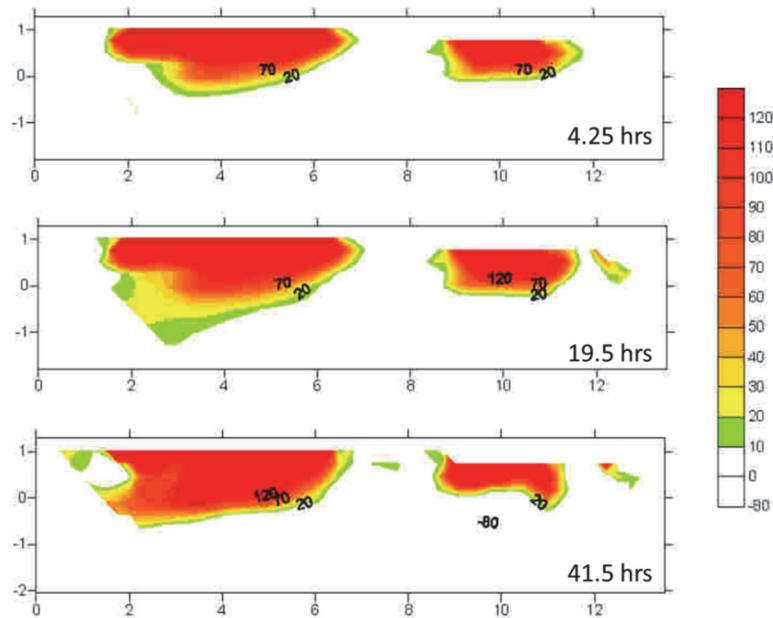
Figure 5. Vertical profile (vertical axis is elevation in m) of percent difference in electrical resistivity of the upgradient electrical resistivity line. The upgradient line was located through the center of the 3×3β plot (left) and the 1×1β plot (right) at the Barren Fork Creek site (fig. 2). The horizontal axis is the distance in m along the electrical resistivity line. Time is the elapsed time from the onset of infiltration.
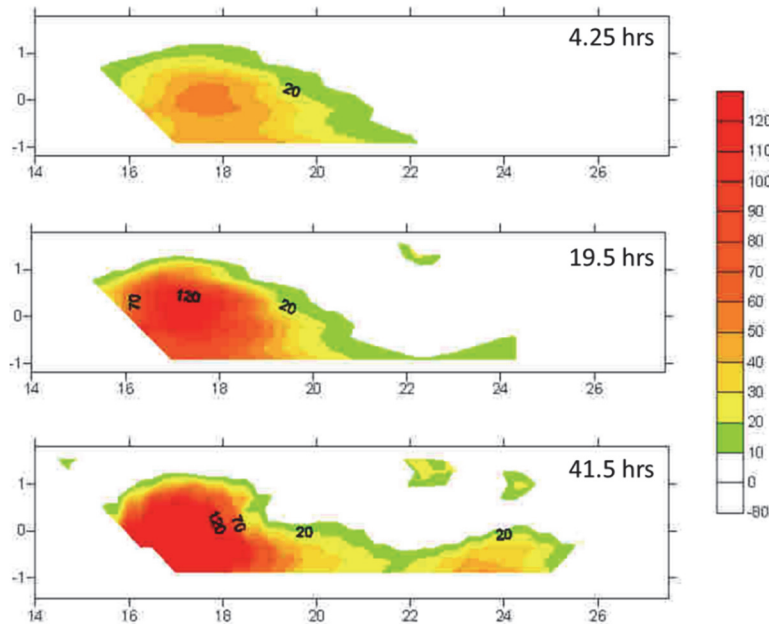

Figure 6. Vertical profile (vertical axis is elevation in m) of percent difference in electrical resistivity of the downgradient electrical resistivity line. The downgradient line was located 3 m downgradient of the center of the 3×3β plot (left) and the 1×1β plot (right) at the Barren Fork Creek site (fig. 2). The horizontal axis is the distance in m along the electrical resistivity line. Time is the elapsed time from the onset of infiltration.

For one plot with a 110 cm layer of silt loam topsoil, the maximum solute transport velocity for SRP, a highly sorbing solute, was 11 times greater than the mean pore water velocity, indicating the striking impact of macropore flow. This research highlighted the difference between the conceptual infiltration model of a diffuse wetting front and actual infiltration in field conditions (Beven and Germann, 2013).

Previous research demonstrated that P transport through gravel alluvial aquifers to streams is significant (Mittelstet et al., 2011), and this research shows that P transport from the soil surface (e.g., fertilizer) to the alluvial aquifer can also be

significant. Because floodplains are hydrologically well-connected to alluvial aquifers and streams in gravelly watersheds, a higher level of agricultural stewardship should be considered for floodplains than for upland areas. This has implications for the development of best management practices for floodplains with gravel aquifers and gravel-bed rivers. Future research should include numerical modeling of these field data in order to estimate long-term P loads to the alluvial aquifers. Additional field testing is needed to generate parameter sets to be able to model P leaching for a wide array of soil conditions.

REFERENCES

Abou Najm, M. R., Jabro, J. D., Iversen, W. M., Mohtar, R. H., & Evans, R. G. (2010). New method for the characterization of three-dimensional preferential flow paths in the field. *Water Resour. Res., 46*(2), W02503. https://dx.doi.org/10.1029/2009WR008594

Akay, O., Fox, G. A., & Simunek, J. (2008). Numerical simulation of flow dynamics during macropore/subsurface drain interactions using HYDRUS. *Vadose Zone J., 7*(3), 909-918. https://dx.doi.org/10.2136/vzj2007.0148

Arkansas v. Oklahoma. (1992). Arkansas et al. v. Oklahoma et al., 503 U.S. 91. Docket No. 90-1262. Washington, DC: U.S. Supreme Court.

Beauchemin, S., & Simard, R. R. (1999). Soil phosphorus saturation degree: Review of some indices and their suitability for P management in Quebec, Canada. *Canadian J. Soil Sci., 79*(4), 615-625. https://dx.doi.org/10.4141/S98-087

Beck, M. A., Zelazny, L. W., Daniels, W. L., & Mullins, G. L. (2004). Using the Mehlich-1 extract to estimate soil phosphorus saturation for environmental risk assessment. *SSSA J., 68*(5), 1762-1771. https://dx.doi.org/10.2136/sssaj2004.1762

Bero, N. J., Ruark, M. D., & Lowery, B. (2016). Bromide and chloride tracer application to determine sufficiency of plot size and well depth placement to capture preferential flow and solute leaching. *Geoderma, 262*, 94-100. http://dx.doi.org/10.1016/j.geoderma.2015.08.001

Beven, K., & Germann, P. (2013). Macropores and water flow in soils revisited. *Water Resour. Res., 49*(6), 3071-3092. https://dx.doi.org/10.1002/wrcr.20156

Clark, G. M., Mueller, D. K., & Mast, M. A. (2000). Nutrient concentrations and yields in undeveloped stream basins of the U.S. *JAWRA, 36*(4), 849-860. https://dx.doi.org/10.1111/j.1752-1688.2000.tb04311.x

Daniel, T. C., Sharpley, A. N., & Lemunyon, J. L. (1998). Agricultural phosphorus and eutrophication: A symposium overview. *J. Environ. Qual., 27*(2), 251-257. https://dx.doi.org/10.2134/jeq1998.00472425002700020002x

DeLaune, P. B., Moore, P. A., Carman, D. K., Sharpley, A. N., Haggard, B. E., & Daniel, T. C. (2004). Development of a phosphorus index for pastures fertilized with poultry litter: Factors affecting phosphorus runoff. *J. Environ. Qual., 33*(6), 2183-2191. https://dx.doi.org/10.2134/jeq2004.2183

Djodjic, F., Katarina, B., & Bergstrom, L. (2004). Phosphorus leaching in relation to soil type and soil phosphorus content. *J. Environ. Qual., 33*(2), 678-684. https://dx.doi.org/10.2134/jeq2004.6780

Fox, G. A., & Penn, C. J. (2013). Empirical model for quantifying total phosphorus reduction by vegetative filter strips. *Trans. ASABE, 56*(4), 1461-1469. http://dx.doi.org/10.13031/trans.56.10133

Fox, G. A., Heeren, D. M., Miller, R. B., Mittelstet, A. R., & Storm, D. E. (2011). Flow and transport experiments for a streambank seep originating from a preferential flow pathway. *J. Hydrol., 403*(3-4), 360-366. http://dx.doi.org/10.1016/j.jhydrol.2011.04.014

Fuchs, J. W., Fox, G. A., Storm, D. E., Penn, C. J., & Brown, G. O. (2009). Subsurface transport of phosphorus in riparian floodplains: Influence of preferential flow paths. *J. Environ. Qual., 38*(2), 473-484. https://dx.doi.org/10.2134/jeq2008.0201

Gburek, W. J., Barberis, E., Haygarth, P. M., Kronvang, B., & Stamm, C. (2005). Phosphorus mobility in the landscape. In J. T. Sims, & A. N. Sharpley (Eds.), *Phosphorus: Agriculture and the environment* (pp. 941-979). Madison, WI: ASA-CSSA-SSSA.

Haggard, B. E. (2010). Phosphorus concentrations, loads, and sources within the Illinois River drainage area, northwest Arkansas, 1997-2008. *J. Environ. Qual., 39*(6), 2113-2120. https://dx.doi.org/10.2134/jeq2010.0049

Halihan, T., Paxton, S., Graham, I., Fenstemaker, T., & Riley, M. (2005). Post-remediation evaluation of a LNAPL site using electrical resistivity imaging. *J. Environ. Monit., 7*(4), 283-287. https://dx.doi.org/10.1039/B416484A

Heeren, D. M., Fox, G. A., & Storm, D. E. (2014a). Technical note: Berm method for quantification of infiltration and leaching at the plot scale in high-conductivity soils. *J. Hydrol. Eng., 19*(2), 457-461. https://dx.doi.org/10.1061/(ASCE)HE.1943-5584.0000802

Heeren, D. M., Fox, G. A., & Storm, D. E. (2015). Heterogeneity of infiltration rates in alluvial floodplains as measured with a berm infiltration technique. *Trans. ASABE, 58*(3), 733-745. https://dx.doi.org/10.13031/trans.58.11056

Heeren, D. M., Fox, G. A., Fox, A. K., Storm, D. E., Miller, R. B., & Mittelstet, A. R. (2014b). Divergence and flow direction as indicators of subsurface heterogeneity and stage-dependent storage in alluvial floodplains. *Hydrol. Proc., 28*(3), 1307-1317. https://dx.doi.org/10.1002/hyp.9674

Heeren, D. M., Fox, G. A., Miller, R. B., Storm, D. E., Fox, A. K., Penn, C. J., ... Mittelstet, A. R. (2011). Stage-dependent transient storage of phosphorus in alluvial floodplains. *Hydrol. Proc., 25*(20), 3230-3243. https://dx.doi.org/10.1002/hyp.8054

Heeren, D. M., Miller, R. B., Fox, A. K., Storm, D. E., Halihan, T., & Penn, C. (2010). Preferential flow effects on subsurface contaminant transport in alluvial floodplains. *Trans. ASABE, 53*(1), 127-136. https://dx.doi.org/10.13031/2013.29511

Kleinman, P. J., Sharpley, A. N., Wolf, A. M., Beegle, D. B., & Moore, P. A. (2002). Measuring water-extractable phosphorus in manure as an indicator of phosphorus in runoff. *SSSA J., 66*(6), 2009-2015. https://dx.doi.org/10.2136/sssaj2002.2009

Maguire, R. O., & Sims, J. T. (2002). Soil testing to predict phosphorus leaching. *J. Environ. Qual., 31*(5), 1601-1609. https://dx.doi.org/10.2134/jeq2002.1601

McKeague, J. A., & Day, J. H. (1966). Dithionite- and oxalate-extractable Fe and Al as aids in differentiating various classes of soils. *Canadian J. Soil Sci., 46*(1), 13-22. https://dx.doi.org/10.4141/cjss66-003

McNeill, J. D. (1980). Electrical conductivity of soils and rocks.

Technical Note TN-5. Mississauga, Ontario, Canada: Geonics.

Mehlich, A. (1984). Mehlich 3 soil test extractant: A modification of Mehlich 2 extractant. *Commun. Soil Sci. Plant Anal., 15*(12), 1409-1416. https://dx.doi.org/10.1080/00103628409367568

Miller, R. B., Heeren, D. M., Fox, G. A., Halihan, T., & Storm, D. E. (2016). Heterogeneity influences on stream water - groundwater interactions in a gravel-dominated floodplain. *Hydrol. Sci. J., 61*(4), 741-750. https://dx.doi.org/10.1080/02626667.2014.992790

Miller, R. B., Heeren, D. M., Fox, G. A., Halihan, T., Storm, D. E., & Mittelstet, A. R. (2014). The hydraulic conductivity structure of gravel-dominated vadose zones within alluvial floodplains. *J. Hydrol., 513*, 229-240. http://dx.doi.org/10.1016/j.jhydrol.2014.03.046

Miller, R. B., Heeren, D. M., Fox, G. A., Storm, D. E., & Halihan, T. (2011). Design and application of a direct-push vadose zone gravel permeameter. *Ground Water, 49*(6), 920-925. https://dx.doi.org/10.1111/j.1745-6584.2010.00796.x

Mittelstet, A. R., Heeren, D. M., Fox, G. A., Storm, D. E., White, M. J., & Miller, R. B. (2011). Comparison of subsurface and surface runoff phosphorus transport rates in alluvial floodplains. *Agric. Ecosyst. Environ., 141*(3-4), 417-425. http://dx.doi.org/10.1016/j.agee.2011.04.006

Murphy, J., & Riley, J. P. (1962). A modified single-solution method for the determination of phosphate in natural waters. *Anal. Chim. Acta, 27*, 31-36. http://dx.doi.org/10.1016/S0003-2670(00)88444-5

Nelson, N. O., Parsons, J. E., & Mikkelsen, R. L. (2005). Field-scale evaluation of phosphorus leaching in acid sandy soils receiving swine waste. *J. Environ. Qual., 34*(6), 2024-2035. https://dx.doi.org/10.2134/jeq2004.0445

Pautler, M. C., & Sims, J. T. (2000). Relationships between soil test phosphorus, soluble phosphorus, and phosphorus saturation in Delaware soils. *SSSA J., 64*(2), 765-773. https://dx.doi.org/10.2136/sssaj2000.642765x

Penn, C., Heeren, D. M., Fox, G. A., & Kumar, A. (2014). Application of isothermal calorimetry to phosphorus sorption onto soils in a flow-through system. *SSSA J., 78*(1), 147-156. https://dx.doi.org/10.2136/sssaj2013.06.0239

Pierzynski, G. M., McDowell, R. W., & Sims, J. T. (2005). Chemistry, cycling, and potential movement of inorganic phosphorus in soils. In J. T. Sims, & A. N. Sharpley (Eds.), *Phosphorus: Agriculture and the environment*. Agronomy Monograph No. 46. Madison, WI: ASA.

Popov, V. H., Cornish, P. S., & Sun, H. (2006). Vegetated biofilters: The relative importance of infiltration and adsorption in reducing loads of water-soluble herbicides in agricultural runoff. *Agric. Ecosyst. Environ., 114*(2-4), 351-359. http://dx.doi.org/10.1016/j.agee.2005.11.010

Reichenberger, S., Bach, M., Skitschak, A., & Frede, H.-G. (2007). Mitigation strategies to reduce pesticide inputs into ground- and surface water and their effectiveness: A review. *Sci. Total Environ., 384*(1-3), 1-35. http://dx.doi.org/10.1016/j.scitotenv.2007.04.046

Sabbagh, G. J., Fox, G. A., Kamanzi, A., Roepke, B., & Tang, J.-Z. (2009). Effectiveness of vegetative filter strips in reducing pesticide loading: Quantifying pesticide trapping efficiency. *J. Environ. Qual., 38*(2), 762-771. https://dx.doi.org/10.2134/jeq2008.0266

Sauer, T. J., & Logsdon, S. D. (2002). Hydraulic and physical properties of stony soils in a small watershed. *SSSA J., 66*(6), 1947-1956. https://dx.doi.org/10.2136/sssaj2002.1947

Sauer, T. J., Logsdon, S. D., Van Brahana, J., & Murdoch, J. F. (2005). Variation in infiltration with landscape position: Implications for forest productivity and surface water quality. *Forest. Ecol. Mgmt., 220*(1-3), 118-127. http://dx.doi.org/10.1016/j.foreco.2005.08.009

Schroeder, P. D., Radcliffe, D. E., & Cabrera, M. L. (2004). Rainfall timing and poultry litter application rate effects on phosphorus loss in surface runoff. *J. Environ. Qual., 33*(6), 2201-2209. https://dx.doi.org/10.2134/jeq2004.2201

Scott, J. T., Haggard, B. E., Sharpley, A. N., & Romeis, J. J. (2011). Change point analysis of phosphorus trends in the Illinois River (Oklahoma) demonstrates the effects of watershed management. *J. Environ. Qual., 40*(4), 1249-1256. https://dx.doi.org/10.2134/jeq2010.0476

Thomas, G. W., & Phillips, R. E. (1979). Consequences of water movement in macropores. *J. Environ. Qual., 8*(2), 149-152. https://dx.doi.org/10.2134/jeq1979.00472425000800020002x

Ulen, B. (1999). Leaching and balances of phosphorus and other nutrients in lysimeters after application of organic manures or fertilizers. *Soil Use Mgmt., 15*(1), 56-61. https://dx.doi.org/10.1111/j.1475-2743.1999.tb00064.x

West, R. R. (1992). Percolate concentrations of nitrogen and phosphorus in poultry litter-applied soils of eastern Oklahoma. MS thesis. Stillwater, OK: Oklahoma State University, Department of Agronomy.